Uniform Linear Arrays With Optimized Inter-Element Spacing for LOS Massive MIMO

Amirashkan Farsaei, Navid Amani, Rob Maaskant, *Senior Member, IEEE*, Ulf Gustavsson, Alex Alvarado, *Senior Member, IEEE*, and Frans M. J. Willems, *Life Fellow, IEEE*

***Abstract*— In this letter, a uniform linear array (ULA) is proposed for line-of-sight massive multiple-input-multiple-output (MIMO). It is assumed that the number of antennas is fixed. For a given ULA with an arbitrary inter-element spacing, the probability that the correlation among the channel vectors of two users being above a threshold value is derived. The inter-element spacing of the proposed ULA is the one for which the aforementioned probability is minimized. To show the effectiveness of the proposed ULA, simulation results for two scenarios are given for a 64-antenna ULA that serves 6 single-antenna users. By using the proposed ULA instead of conventional half-wavelength ULA, 5th percentile sum-rate for zero-forcing precoder is improved by 9.90 bits/channel use in first scenario without dropping, and by 1.43 bits/channel use in second scenario with dropping 1 user.**

***Index Terms*— Line-of-sight, massive MIMO, uniform linear array, zero-forcing.**

I. Introduction

MASSIVE multiple-input-multiple-output (MIMO) is foreseen as a key enabling technology for fifth-generation wireless networks and beyond [1], [2]. It is shown in [3] that in line-of-sight (LOS) massive MIMO, there is a nonnegligible probability that the channel vectors of some users become highly correlated, which results in a non-favorable propagation environment. The high correlation leads to a reduction in the sum-rates of linear and nonlinear precoders [4, Fig. 5]. The reduction of the sum-rate due to the high correlation is considerable for LOS environments with max-min power control as reported in [5], [6] (max-min power control is used to provide uniformly good service for the users as reported in [3]). In addition, it is shown in [5, Fig. 2] that when there is only one pair of highly correlated users, the signal to noise ratio with max-min power control will drop significantly. To deal with highly correlated scenarios in LOS environments with max-min power control, [3], [5], [6] studied dropping algorithms. However, dropping users may not be desirable in the case of latency-sensitive communication.

To avoid dropping and alleviate a high inter-user correlation, one can increase the aperture size to improve the angular resolution of the base station (BS) antenna array. By increasing the aperture size, the minimum resolvability angular resolution of the array, which is defined by the well-known Rayleigh's criterion [7], is improved. Hence, by employing an inter-element spacing (δ) larger than the conventional $\lambda/2$ (λ is a wavelength) the angular resolution of an array with a fixed number of elements is enhanced [8, Sec. 7.2.4]. The major drawback of increasing δ in the uniform linear arrays (ULAs) is the appearance of grating lobes (beamforming ambiguities) [9], [10]. The grating lobes may cause a high correlation among the channel vectors of users with a large angular separation (not co-located users). To avoid grating lobes, in [11] a maximum allowable δ, depending on the field-of-view (FOV), is proposed, where the increase in the aperture size is minimal for wide FOVs. Increasing δ is reported beneficial in terms of spectral efficiency for a BS antenna array with a fixed number of antennas [12]. A small LOS spectral efficiency improvement is also reported in [10] by deploying ULAs with larger inter-element spacing. However, none of the above-mentioned studies approaches the problem analytically to compute the probability of correlated users in the absence or presence of grating lobes.

In this letter, a ULA for LOS environments is proposed assuming a fixed number of omnidirectional antennas at the BS. We derive the probability that the correlation among the channel vectors of two users being above a threshold for a ULA with an arbitrary inter-element spacing. The inter-element spacing of the proposed ULA is the one for which the aforementioned probability is minimized. The proposed ULA is optimized for the case when there are only two users. For more users, we present simulation results for two different scenarios, to show the effectiveness of the proposed array compared to conventional half-wavelength ULA with a known linear precoder, i.e., zero-forcing (ZF).

II. System Model

We consider a BS equipped with a ULA of M antennas[1] located on the x-axis (see Fig. 1). Two users are assumed to be in the x-y plane, where R_1 and R_2 are the distance from the users to the first element of the array, and ϕ_1 and ϕ_2 are the azimuth angles of the users. It is assumed that ϕ_1 and ϕ_2 are independent random variables that are uniformly distributed in a FoV of $\phi_l \in (\pi/2 - \phi_o, \pi/2 + \phi_o)$, where

[1] Analysis of uniform planar array (3D beamforming) is left for future work.

Manuscript received September 18, 2020; accepted October 7, 2020. Date of publication October 13, 2020; date of current version February 11, 2021. This project has received funding from the European Union's Horizon 2020 research and innovation programme under the Marie Sklodowska-Curie grant agreement No 721732. The associate editor coordinating the review of this letter and approving it for publication was M. C. Aguayo-Torres. *(Corresponding author: Amirashkan Farsaei.)*

Amirashkan Farsaei, Alex Alvarado, and Frans M. J. Willems are with the Department of Electrical Engineering, Eindhoven University of Technology, 5600 MB Eindhoven, The Netherlands (e-mail: a.farsaee@tue.nl; a.alvarado@tue.nl; f.m.j.willems@tue.nl).

Navid Amani and Rob Maaskant are with the Department of Electrical Engineering, Chalmers University of Technology, 412 96 Gothenburg, Sweden (e-mail: anavid@chalmers.se; rob.maaskant@chalmers.se).

Ulf Gustavsson is with Ericsson Research, Ericsson AB, 417 56 Gothenburg, Sweden (e-mail: ulf.gustavsson@ericsson.com).

Digital Object Identifier 10.1109/LCOMM.2020.3030681

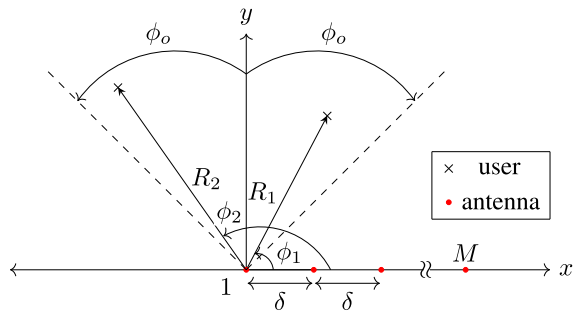

Fig. 1. ULA with M elements on x-axis with inter-element spacing δ. The distance between the first element of the array and the users are R_1 and R_2.

$\phi_o \in (0, \pi/2)$. The channel between user l ($l \in \{1, 2\}$) and antenna m ($m \in \{1, 2, \ldots, M\}$) is modeled as [8, Sec. 7.2.2]:

$$h_{lm} = \sqrt{\beta_l} e^{-\jmath k R_l} e^{+\jmath k(m-1)\delta \cos(\phi_l)}, \tag{1}$$

where β_l is the large-scale fading for user l, k is the wavenumber, and δ is the inter-element spacing of ULA. Typically, δ is assumed to be $\lambda/2$. Using (1), the channel vector $\boldsymbol{h}_l = (h_{l1}, h_{l2}, \ldots, h_{lM})^T$ is found. The spatial correlation between the channel vectors $\boldsymbol{h}_1$ and $\boldsymbol{h}_2$ is given by:

$$\rho = \frac{\boldsymbol{h}_2^H \boldsymbol{h}_1}{\|\boldsymbol{h}_1\| \|\boldsymbol{h}_2\|}. \tag{2}$$

We use the term spatial correlation for (2) (following the literature) throughout the letter, although, (2) is the inner-product of normalized $\boldsymbol{h}_1$ and $\boldsymbol{h}_2$ for a given coherence interval. By replacing the elements of the channel vectors $\boldsymbol{h}_1$ and $\boldsymbol{h}_2$ using (1), in (2), $|\rho|$ is found by:

$$|\rho| = \frac{1}{M} \left| \frac{\sin(Mk\frac{\delta}{2}\psi)}{\sin(k\frac{\delta}{2}\psi)} \right|, \tag{3}$$

where $\psi = \cos(\phi_1) - \cos(\phi_2)$. Using (3), $|\rho|$ is expressed as a function of ψ with the inter-element spacing of δ as follows:

$$|\rho| = f_\delta(\psi), \quad \psi \in \left(2\cos(\frac{\pi}{2} + \phi_o), 2\cos(\frac{\pi}{2} - \phi_o)\right). \tag{4}$$

Note $f_\delta(\psi)$ is periodic with period $T = \lambda/\delta$ [8, Sec. 7.2.4].

For a given realization of a channel of two users, assume that the angular separation of the users is $\psi = \Delta$. One can find the inter-element spacing δ_1 such that the users become orthogonal, i.e., $|\rho| = f_{\delta_1}(\Delta) = 0$. Suppose the users move and the angular separation of the users becomes $\Delta' \neq \Delta$. In this case, another inter-element spacing $\delta_2 \neq \delta_1$ has to be used to make the users orthogonal. However, changing the inter-element spacing for each realization of users is not practical. Therefore, a probabilistic approach is required to find the best inter-element spacing $\delta^\star$ for which a small $|\rho|$ is achieved with a high probability. In other words, the best inter-element spacing is the one that has the minimum probability that $|\rho|$ becomes larger than a given threshold ρ_o. We use the following definition for the rest of the letter.

Definition 1: The probability that a pair of users with the spatial correlation of ρ become correlated with a given ρ_o, is denoted by p, and defined as:

$$p \triangleq \Pr\{|\rho| > \rho_o\}. \tag{5}$$

Appropriate probability analysis is required to find the inter-element spacing for the case of two users for which p is minimized, which is given in the sequel.

III. Probability Analysis

In this section, we find p for ULAs with $\delta = \lambda/2$ and then for ULAs with $\delta > \lambda/2$ when there are only two users.

A. ULAs With $\delta = \lambda/2$

In Fig. 2, $|\rho| = f_{\lambda/2}(\psi)$ is shown for a ULA of $M = 10$ antennas. The shaded areas show when user 1 and user 2 become correlated with a given $\rho_o = 0.64$ ($\rho_o = 0.64$ is the 3-dB point [9, Sec. 6.3]) or equivalently a given ψ_o. If ψ_o is chosen as in Fig. 2, we can derive p as follows using the periodicity of $f_{\lambda/2}(\psi)$ ($T = 2$):

$$p = \Pr\{|\psi| < \psi_o\} + \Pr\{2 - \psi_o < |\psi| < 2\} = \alpha_0 + \alpha_1, \tag{6}$$

where the corresponding area for α_0 and α_1 are shown in Fig. 3 by the blue and yellow shaded area, respectively. We find α_0 as follows:

$$\begin{aligned}\alpha_0 &= \Pr\{|\psi| < \psi_o\} = 2\Pr\{0 \le \psi < \psi_o\} \\ &= 2\Pr\{0 \le \cos(\phi_1) - \cos(\phi_2) < \psi_o\} \\ &= 2\Pr\{\cos(\phi_2) \le \cos(\phi_1) < \cos(\phi_2) + \psi_o\} \\ &= 2\Pr\{\cos^{-1}(\cos(\phi_2) + \psi_o) < \phi_1 \le \phi_2\}. \end{aligned} \tag{7}$$

By using the same approach, α_1 is found by:

$$\begin{aligned}\alpha_1 &= \Pr\{2 - \psi_o < |\psi| < 2\} \\ &= 2\Pr\{2 - \psi_o < \psi < 2\} \\ &= 2\Pr\{2 - \psi_o < \cos(\phi_1) - \cos(\phi_2) < 2\} \\ &= 2\Pr\{\cos(\phi_2) + 2 - \psi_o < \cos(\phi_1) < \cos(\phi_2) + 2\}. \end{aligned} \tag{8}$$

Note $\cos(\phi_2) + 2 > 1$ for all ϕ_2 in the FoV. Therefore:

$$\begin{aligned}\alpha_1 &= 2\Pr\{\cos(\phi_2) + 2 - \psi_o < \cos(\phi_1) < 1\} \\ &= 2\Pr\left\{\frac{\pi}{2} - \phi_o < \phi_1 < \cos^{-1}(\cos(\phi_2) + 2 - \psi_o)\right\}. \end{aligned} \tag{9}$$

Recall that ϕ_l with $l = 1, 2$ are uniformly distributed in the FoV. Consequently, given (7)–(9), α_0 and α_1 are found by evaluating the following integrals:

$$\alpha_0 = 2\int_{\frac{\pi}{2}-\phi_o}^{\frac{\pi}{2}+\phi_o} \frac{1}{2\phi_o} \int_{\cos^{-1}(\cos(\phi_2)+\psi_o)}^{\phi_2} \frac{1}{2\phi_o} d\phi_1 d\phi_2, \tag{10}$$

$$\alpha_1 = 2\int_{\frac{\pi}{2}-\phi_o}^{\frac{\pi}{2}+\phi_o} \frac{1}{2\phi_o} \int_{\frac{\pi}{2}-\phi_o}^{\cos^{-1}(\cos(\phi_2)+2-\psi_o)} \frac{1}{2\phi_o} d\phi_1 d\phi_2. \tag{11}$$

Whenever ρ_o is higher than the black squares (first side-lobes at $\rho_o = 2/(3\pi)$ [9, Sec. 6.3]) shown in Fig. 2, p can be written as a sum of α_0 and α_1 in (6), where α_0 and α_1 are found by (10) and (11), respectively.

B. ULAs With $\delta > \lambda/2$

In this section, we first find p for a ULA with $\delta = \lambda$. Then, we give an expression for ULAs with any $\delta > \lambda/2$. In Fig. 3, $|\rho| = f_\lambda(\psi)$ is shown for a ULA of $M = 10$ antennas. The shaded areas show when user 1 and user 2 become correlated with a given ρ_o. The probability p is found by:

$$\begin{aligned}p &= \Pr\{|\rho| > \rho_o\} \\ &= \Pr\{|\psi| < \psi_o\} + \Pr\{1 - \psi_o < |\psi| < 1 + \psi_o\} \\ &\quad + \Pr\{2 - \psi_o < |\psi| < 2\} = \alpha_0 + \alpha_1 + \alpha_2, \end{aligned} \tag{12}$$

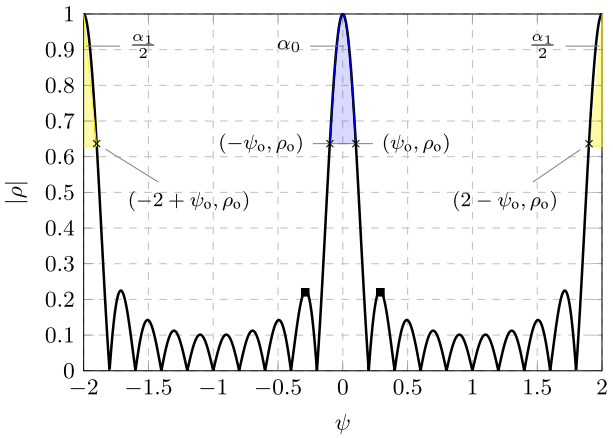

Fig. 2. The function $|\rho| = f_{\lambda/2}(\psi)$ for a ULA with $M = 10$ and $\psi_o = 0.1$ ($\rho_o = 0.64$) for a FoV of $(0, \pi)$.

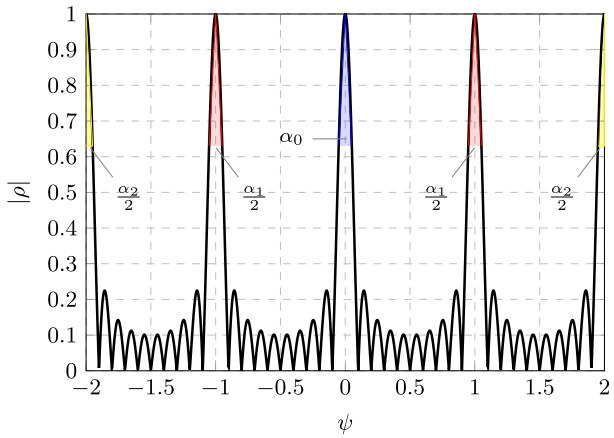

Fig. 3. The function $|\rho| = f_{\lambda}(\psi)$ for $M = 10$, $\rho_o = 0.64$, $\psi_o = 0.05$, and for a FoV of $(0, \pi)$. The blue, red, and yellow shaded area are associated with α_0, α_1, and α_2, respectively. Note that $T = 1$.

where the corresponding area for α_0, α_1, and α_2 are shown in Fig. 3 by blue, red, and yellow shaded area, respectively. Similar to case of $\delta = \lambda/2$, we find integrals for α_0, α_1, and α_2. For a ULA with $\delta > \lambda/2$, p for a given ρ_o is found by:

$$p = \Pr\{|\rho| > \rho_o\} = \Pr\{|\psi| < \psi_o\} + \sum_{i=1}^{n} \Pr\{iT - \psi_o < |\psi| < iT + \psi_o\} = \alpha_0 + \sum_{i=1}^{n} \alpha_i, \quad (13)$$

where n is the number of areas where $\psi > 0$ and $\rho > \rho_o$ excluding the area corresponds to α_0. For instance, $n = 2$ for $\delta = \lambda$. We numerically evaluate integrals to find α_0 and α_i to find p, same as the analysis done for $\lambda/2$.

In Fig. 4, p is shown as a function of δ/λ for $M = 10, 20, 64$ for $\delta \leq 2.5\lambda$,[2] $\rho_o = 0.64$ for a FoV of $(0, \pi)$. For each M, $\delta^\star$ shows the inter-element spacing with minimum p, and there are three local minima as shown by colored circles δ_{n_1}, δ_{n_2}, and δ_{n_3}. By increasing δ, p is continuously increasing and then decreasing with decaying behavior. There are two reasons for explaining this behavior. First, by increasing δ, the angular resolution of the array is improved (compare the shaded blue area in Fig. 2 and Fig. 3), which decreases p. Second, by increasing δ, the grating lobes (the peaks correspond to $\alpha_i, i \neq 0$, see Fig. 3) gradually appear in the FoV, which increases p. Due to the first reason, p should decrease, and due to the second reason, p should increase. As can be seen, we see a more decrease in p, which shows that increasing the angular resolvability has a stronger effect on p than the grating lobes. Moreover, the effect of increasing the angular resolvability and the appearance of grating lobes is decaying as δ approaches 2.5λ. We further observe that in all the scenarios, p curves approach $p = 1/M$ (horizontal dash-dotted lines).

We approximate δ_{n_i} by the inter-element spacing for which the shaded area associated with $(i+1)$th grating lobe appeared in function $f_\delta(\psi)$ (e.g., in Fig. 3, the yellow shaded area is associated with the 2nd grating lobe). For instance, δ_{n_1} is approximated by the inter-element spacing for which the yellow area starts to appear in Fig. 3. For a given ψ_o, we approximate δ_{n_i} by solving $\psi_o - (i+1)\lambda/\delta = -2$ for δ, which leads to $\delta_{n_i} \approx \lambda(2M(i+1) - 1)/4M$ for ψ_o of

[2]The choice of 2.5λ is arbitrary to limit the maximum aperture size.

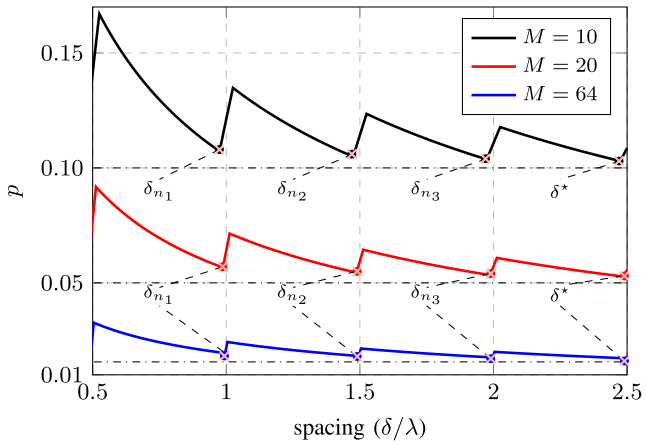

Fig. 4. The probability p ($\rho_o = 0.64$) as a function of δ/λ for $M = 10, 20, 64$ for a FoV of $(0, \pi)$ for $\delta \in [0.5\lambda, 2.5\lambda]$. For each M, the minimum p occurs at $\delta^\star$. The local minima are δ_{n_1}, δ_{n_2} and δ_{n_3}.

the scenario in Fig. 4. The results in Fig. 4 shows that the approximations of δ_{n_i} (pink cross) match with the numerical values of δ_{n_i} (colored circle). For a given M, we propose to use $\delta^\star$, which is the inter-element spacing with the minimum p. To reduce the aperture size, one can use $\delta_{n_i}, i = 1, 2, 3$ instead of $\delta^\star$. We assume a narrow-band communication system in this letter. However, the results in Fig. 4 can be used for multi sub-carriers systems. By choosing an appropriate spacing for the center sub-carrier, one can make p smaller than a threshold for all the sub-carriers. The performance of using δ_{n_1} and $\delta^\star$ for more number of users is compared in the next Section. Regarding scenarios where there are paths other than LOS path some insights can be found in [13].

IV. Simulation Results

In this section, the performance of ULAs with $\delta^\star$ and δ_{n_1} (see Fig. 4) are compared with half-wavelength ULA for FoV of $(0, \pi)$ in LOS massive MIMO with max-min power control. To study the worst-case scenarios, the users are assumed to be at the cell-edge (no shadowing), which is assumed to be at the far-field of the array. We compare the arrays qualitatively and quantitatively as follows. First, qualitatively, for a given ρ_o, we compare the probability that at least there is one correlated

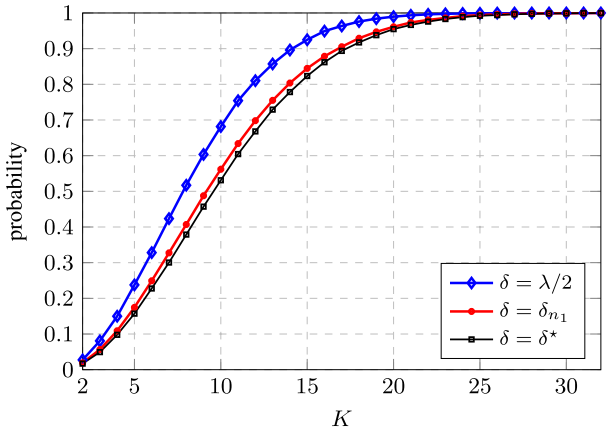

Fig. 5. The probability that there is at least one pair of correlated users for $\delta = \lambda/2$, δ_{n_1}, $\delta^\star$ when $M = 64$, $\rho_o = 0.64$ for a FoV of $(0, \pi)$.

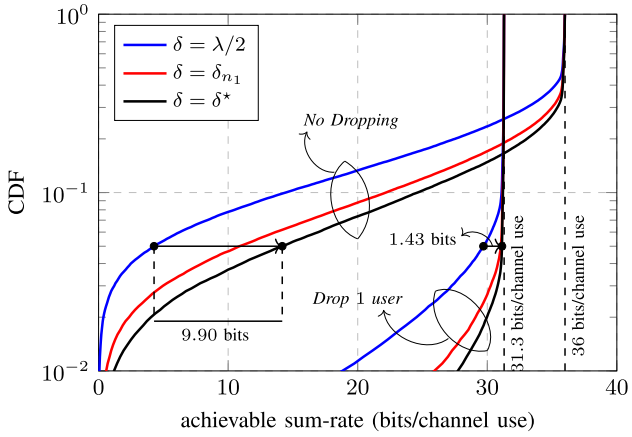

Fig. 6. The CDF plots of ZF sum-rate for $\delta = \lambda/2$, δ_{n_1}, $\delta^\star$ for two different scenarios, i.e., *No dropping* and *Drop* 1 *user* (based on the algorithm of [3]). The horizontal arrow shows the 5th percentile improvement of the sum-rate by using $\delta^\star$ instead of $\delta = \lambda/2$. The vertical dashed lines show the ZF sum-rate in FP for the two scenarios.

pair of users as a function of the number of users for the three arrays. Second, quantitatively, we compare cumulative distribution function (CDF) of ZF sum-rates of the arrays.

In Fig. 5, for a ULA with $M = 64$ antennas, the probability that there is at least one pair of correlated users ($\rho_o = 0.64$) is shown as a function of the number of users K for $\delta = \lambda/2$ (blue), δ_{n_1} (red), and $\delta^\star$ (black). For a given number of users, the ULA with $\delta^\star$ has a smaller probability compared to $\lambda/2$, which means it has a better ability to decorrelate the channel vectors of the users. By using δ_{n_1} instead of $\delta^\star$, we can reduce the aperture size, while the probability that there is at least one pair of correlated users is not that higher than that of $\delta^\star$.

In Fig. 6, the CDF of ZF sum-rate is shown for the arrays with $K = 6$ and $M = 64$ in two different scenarios, where 100K realizations of users' locations are drawn for each scenario. In the first scenario, no user is dropped (*No Dropping*), while in the second scenario one user is dropped (*Drop* 1 *user*) based on the dropping algorithm of [3]. The transmit power at the BS is fixed and is the same in both scenarios such that in the favorable propagation (FP) [14] (when the users are mutually orthogonal), a sum-rate of 36 bits/channel use is achieved in the first scenario, and a sum-rate of 31.3 bits/channel use is achieved in the second scenario (see the vertical dashed lines in Fig. 6). When no user is dropped, by employing the proposed array (black), the 5th percentile sum-rate is improved significantly (9.90 bits/channel use) compared to that of the ULA with $\delta = \lambda/2$ (blue). This improvement becomes 1.43 bits/channel use when 1 user is dropped. By dropping 1 user, the 5th percentile ZF sum-rate of all the arrays is improved significantly, which shows it is necessary to drop 1 user. To reduce the aperture size, the array with δ_{n_1} (red) can be used instead of $\delta^\star$ with a loss in performance, i.e., 3.30 bits/channel use loss in *No Dropping* scenario and 0.09 bits/channel use in *Drop* 1 *user* scenario.

V. Conclusion

In this letter, we use probability analysis to find an improved uniform linear array for LOS massive MIMO. For the case of two users, the proposed ULA has the minimum probability that the correlation of the users being above a given threshold. For more users, we present the simulation results for a known linear precoder, i.e., ZF to show the effectiveness of the proposed ULA compared to half-wavelength ULA.

References

[1] T. L. Marzetta, "Noncooperative cellular wireless with unlimited numbers of base station antennas," *IEEE Trans. Wireless Commun.*, vol. 9, no. 11, pp. 3590–3600, Nov. 2010.
[2] E. G. Larsson, O. Edfors, F. Tufvesson, and T. L. Marzetta, "Massive MIMO for next generation wireless systems," *IEEE Commun. Mag.*, vol. 52, no. 2, pp. 186–195, Feb. 2014.
[3] H. Yang and T. L. Marzetta, "Massive MIMO with max-min power control in line-of-sight propagation environment," *IEEE Trans. Commun.*, vol. 65, no. 11, pp. 4685–4693, Nov. 2017.
[4] X. Gao, O. Edfors, F. Rusek, and F. Tufvesson, "Linear pre-coding performance in measured very-large MIMO channels," in *Proc. IEEE Veh. Technol. Conf. (VTC Fall)*, Sep. 2011, pp. 1–5.
[5] A. Farsaei, A. Alvarado, F. M. J. Willems, and U. Gustavsson, "An improved dropping algorithm for line-of-sight massive MIMO with max-min power control," *IEEE Commun. Lett.*, vol. 23, no. 6, pp. 1109–1112, Jun. 2019.
[6] A. Farsaei, A. Alvarado, F. M. J. Willems, and U. Gustavsson, "An improved dropping algorithm for Line-of-Sight massive MIMO with Tomlinson–Harashima precoding," *IEEE Commun. Lett.*, vol. 23, no. 11, pp. 2099–2103, Nov. 2019.
[7] E. Hecht, *Optics* (Pearson Education). Reading, MA, USA: Addison-Wesley, 2002.
[8] D. Tse and P. Viswanath, *Fundamentals of Wireless Communication*. New York, NY, USA: Cambridge University Press, May 2005.
[9] C. A. Balanis, *Antenna Theory: Analysis and Design*. Hoboken, NJ, USA: Wiley, 2016.
[10] S. Pratschner, E. Zochmann, H. Groll, S. Caban, S. Schwarz, and M. Rupp, "Does a large array aperture pay off in line-of-sight massive MIMO?" in *Proc. IEEE 20th Int. Workshop Signal Process. Adv. Wireless Commun. (SPAWC)*, Jul. 2019, pp. 1–5.
[11] N. Amani, A. A. Glazunov, M. V. Ivashina, and R. Maaskant, "Per-antenna power distribution of a zero-forcing beamformed ULA in pure LOS MU-MIMO," *IEEE Commun. Lett.*, vol. 22, no. 12, pp. 2515–2518, Dec. 2018.
[12] D. Pinchera, M. Migliore, F. Schettino, and G. Panariello, "Antenna arrays for line-of-sight massive MIMO: Half wavelength is not enough," *Electronics*, vol. 6, no. 3, p. 57, Aug. 2017.
[13] N. Amani *et al.*, "Array configuration effect on the spatial correlation of MU-MIMO channels in NLoS environments," in *Proc. 14th Eur. Conf. Antennas Propag. (EuCAP)*, Mar. 2020, pp. 1–4.
[14] H. Q. Ngo, E. G. Larsson, and T. L. Marzetta, "Aspects of favorable propagation in massive MIMO," in *Proc. 22nd Eur. Signal Process. Conf. (EUSIPCO)*, Sep. 2014, pp. 76–80.